Automating Stochastic Antibody-Drug Conjugation: A Self-Driving Lab Approach for Enhanced Therapeutic Development

Liam Roberts,[a] Matthew E. Reish,[b] Jerrica Yang,[a] Wenyu Zhang,[a] Joshua S. Derasp*[a] and Jason E. Hein*[a,b,c,d]

[a.] *Department of Chemistry, The University of British Columbia, Vancouver, BC V6T 1Z1, Canada*
[b.] *Department of Chemistry, University of Bergen, Norway*
[c.] *Acceleration Consortium, University of Toronto, Toronto, ON, Canada*
[d.] *Telescope Innovations Corp., Vancouver, BC, Canada*

Contents

General remarks

This supplementary information includes detailed information on the development and implementation of an automated stochastic conjugation platform. All experiments were performed using existing resources in our lab. Unless otherwise mentioned, all chemicals were bought from conventional suppliers and used as received. The rationale behind decisions made in terms of chemicals and equipment used is explicitly stated in the following remarks or the research paper. Code availability found in https://gitlab.com/heingroup/adc-automation. Hardware design files are found in https://gitlab.com/heingroup/adc-automation-hardware.

Chemicals and reagents

Trastuzumab, diluted to 4.2 mg/mL in PBS pH 7.4, was obtained from Selleckchem and kept at 4°C. Tris(2-carboxyethyl) phosphine (TCEP) was sourced from Thermo Fisher Scientific, diluted to 0.2 mM in deionized water (dH2O), and stored at -80°C. Maleimidocaproyl-valine-citrulline-p-aminobenzyloxycarbonyl monomethylauristatin E (vcMMAE) was purchased from AmBeed, diluted to 1 mM in DMSO, and stored at -20°C. Diethylenetriamine pentaacetic acid (DTPA) and PBS pH 7.4 were purchased from Thermo Fisher Scientific. Optima-grade UHPLC solvents were purchased from Thermo Fisher Scientific.

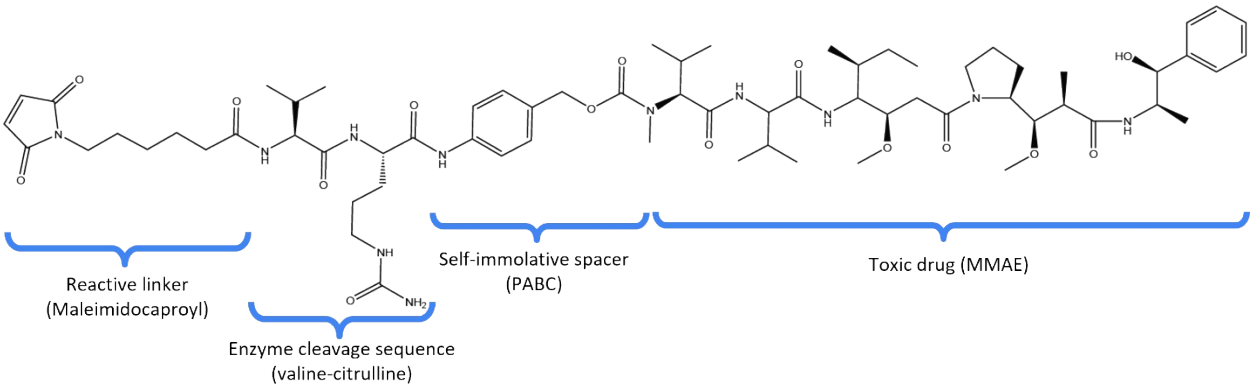

Figure S1. Structure of vcMMAE. The functional regions of vcMMAE are highlighted.

Hardware

Analytical equipment

Hydrophobic interaction chromatography high-performance liquid chromatography (HIC-HPLC) data was acquired on an Agilent 1290 Infinity UHPLC system equipped with a TSKgel Butyl-NPR HIC column (Tosoh Biosciences). Ultraviolet (UV) absorbance of the column eluate was detected by the Agilent 1290 Infinity diode array detector. UV-visible (UV-Vis) analysis for determining antibody and drug-linker yields was conducted with a SpectraMax QuickDrop UV-Vis Spectrophotometer (Molecular Devices).

Automation platform hardware and set up

Design files and firmware for the wireless mobile liquid handler, vacuum filtration apparatus, automated decapper and cap dispenser are found at https://gitlab.com/heingroup/adc-automation-hardware. Python control software for each of the components is included in the main Gitlab project linked above in General Remarks. Annotated images of the full system and custom hardware components are found below.

Full platform description

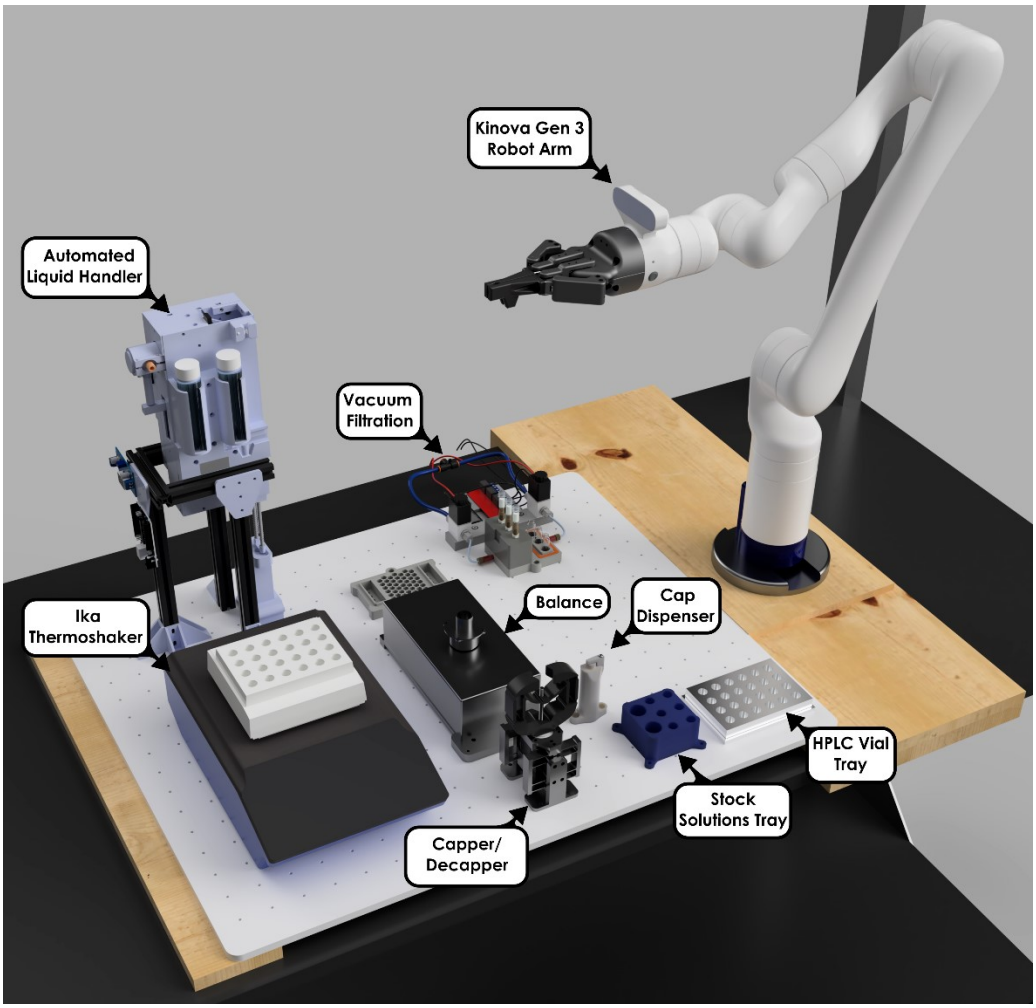

Figure S2. Render of the full robotic system for antibody-drug conjugation with each of the hardware modules labelled.

The experiment is described in detail below in 'Experimental Procedures' with the function of each hardware module described here in brief. The Kinova Gen3 robot arm was used to manipulate HPLC vials, filter blocks, and the automatic liquid handler. 3D printed grippers of the robot arm securely held the liquid handler, filter block, and HPLC vials. We developed an automatic liquid handler in collaboration with Telescope Innovations Corporation. Reagent weights were measured gravimetrically using the Mettler-Toledo WKS204C balance. Decapping and capping of HPLC vials were performed using a custom decapper and caps were dispensed from a custom cap holder, both developed in the lab. Incubations at 37°C and 25°C were conducted using an IKA Matrix Delta Orbital Plus thermo-shaker. For purification, Thermo

Fisher Scientific 0.5 mL 40K Zeba spin desalting columns were used to remove excess reducing agent and drug-linker. The Zeba column purification process incorporated a custom-built vacuum filtration apparatus, connected to an IKA Vacstar vacuum pump. The filter blocks, filter base and parts of the automated liquid handler were produced using a Formlabs Form 3L 3D Printer. The robot gripper, solenoid block, cap dispenser, capper / decapper, liquid handler baser and parts of the liquid handler were all produced using an Ultimaker S6 FDM 3D printer using PLA or Nylon filament.

Automated liquid handler

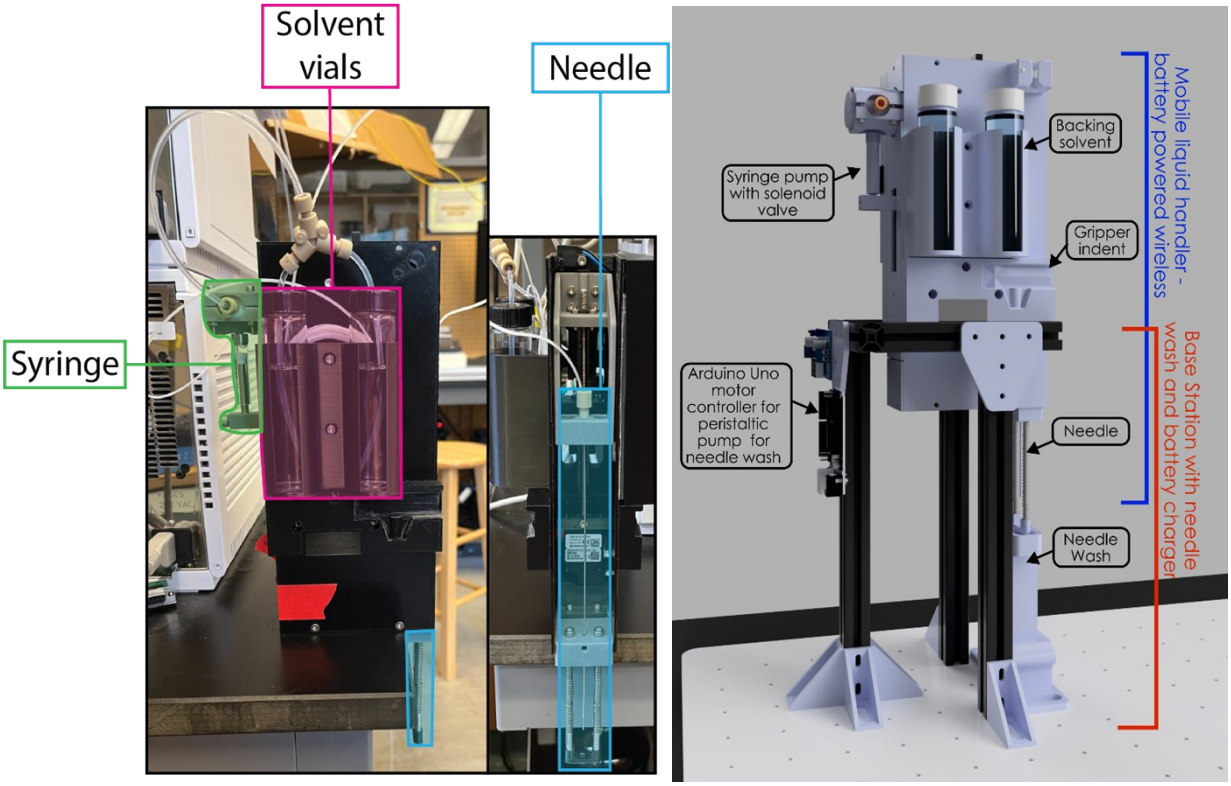

Figure S3. Automated liquid handler. Left: shows front and side view photos of the liquid handler highlighting the syringe pump (green), the solvent vials (magenta) which held PBS pH 7.4 and the needle (blue) which moved vertically to pass through the needle guide and septa. Right: Shows a render of the liquid handler highlighting some of the main design features of the liquid handler.

Table S1. Automatic liquid handler method development.

Test Number	1	2	3	4	5	6
Pause Time[a] (s)	0	3	3	3	3	3

Air Gap Size (µL)	50	100	125	50	50	50
Air Gap Dispensed (%)	30	25	40	90	90	90
Arm Speed (mm/s)	250	250	250	250	10	10
Needle Height[b] (mm)	18	18	18	18	18	-2
Standard Deviation (µL)	2.61	3.96	4.24	2.86	3.62	2.42
Average Error (%)	31.0	32.1	20.5	13.6	18.0	5.7
Replicates[c]	3	4	5	6	10	15

[a]Refers to the pause post-aspiration. [b]Needle height between liquid handling rounds relative to the needle guide (see ESI Fig. 4 for details). [c]Low number of replicates during early rounds of testing as the poor average error indicated a need for adjustments.

In this study, we achieved an acceptable average error to demonstrate the feasibility of our proof-of-concept automated conjugation platform. However, to ensure the consistent production of ADCs with precise DARs, we plan to further enhance the liquid handler, improving both its accuracy and precision.

One of the key challenges in achieving accurate liquid handling at very small volumes is the effect of fluid surface tension. This issue is particularly problematic for manual pipetting but can be mitigated by adjusting technique—such as contacting the side of the vial to break the surface tension of adhered droplets. In future iterations of our robotic platform, we aim to refine positioning to replicate this physical behavior, thereby enhancing precision. Additionally, several design improvements for a future version of the liquid handler are under consideration:

1. Increasing the rigidity of the 3D-printed mechanism that actuates the plunger.

2. Implementing a linear encoder to track the carriage position rather than relying on the linear actuator shaft.

3. Reducing the syringe diameter to enable finer control by allowing more stepper motor steps per delivered volume.

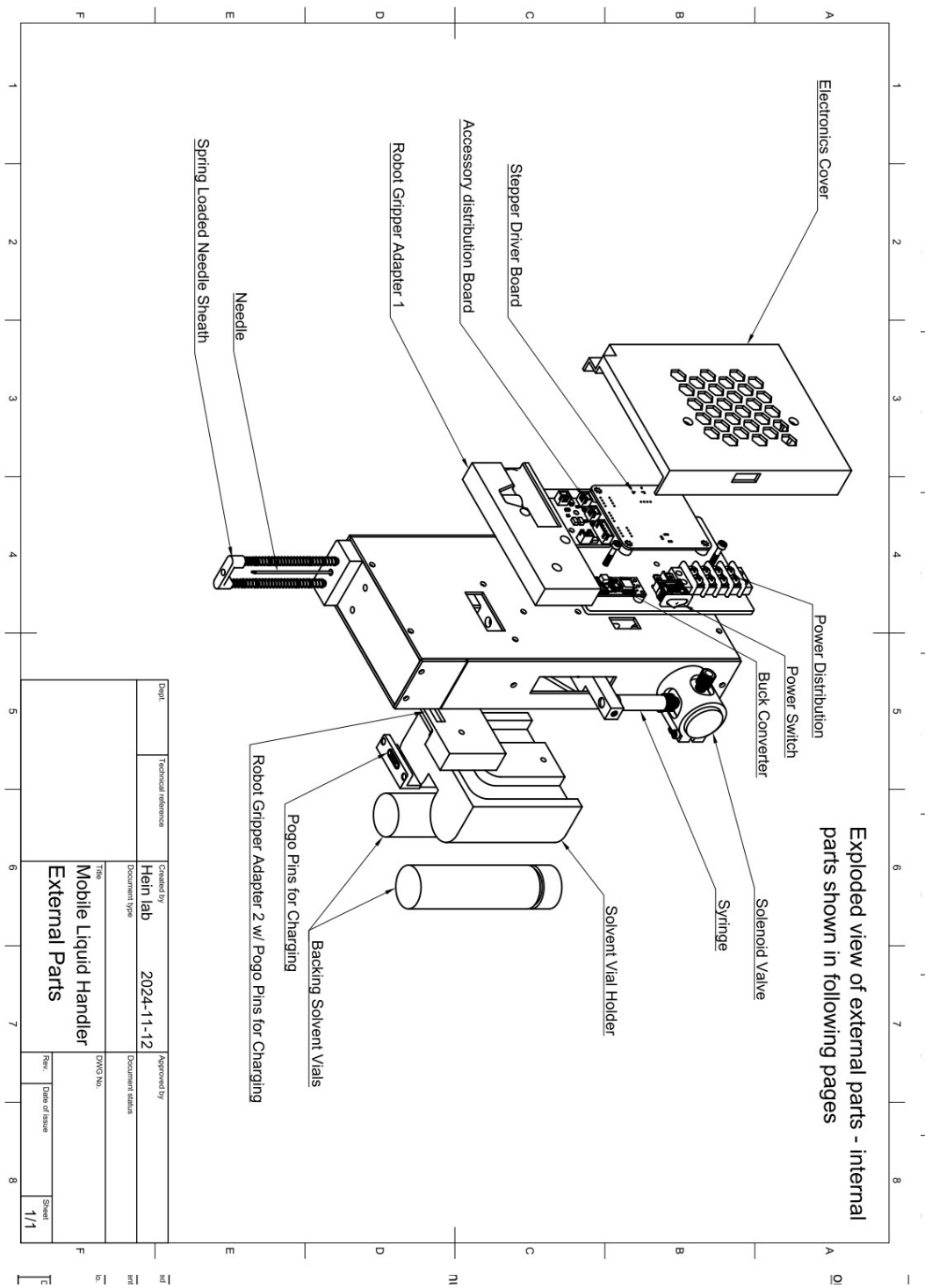

Figure S4. Exploded view of the external components of the automated mobile liquid handler. Internal parts are show below.

Figure S5. Drawing of the internal components of the automated mobile liquid handler.

Figure S6. Drawing of the charging and needle washing base station for the automated mobile liquid handler.

Vacuum filtration apparatus

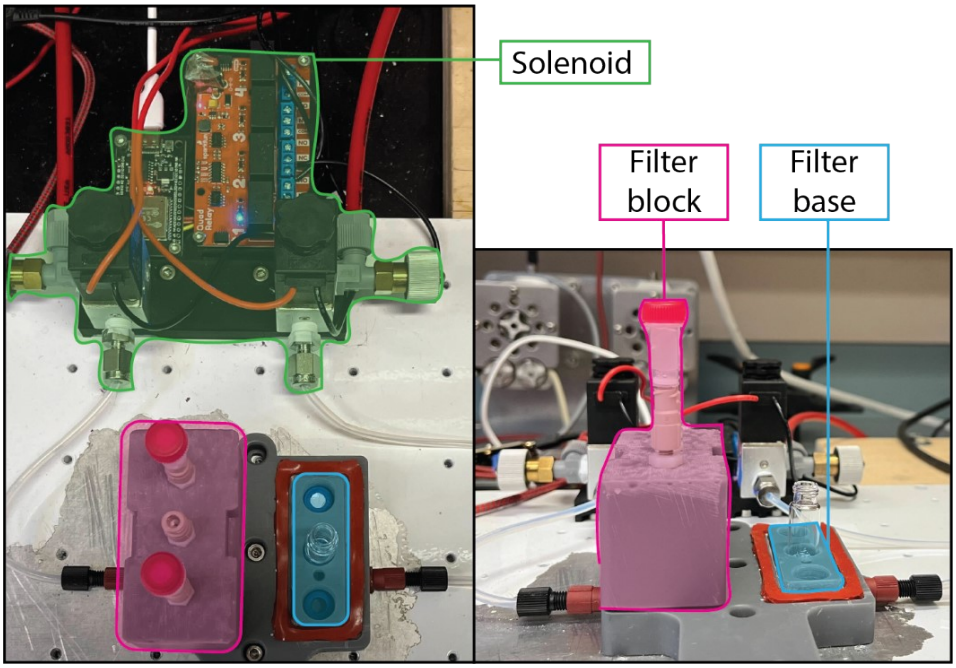

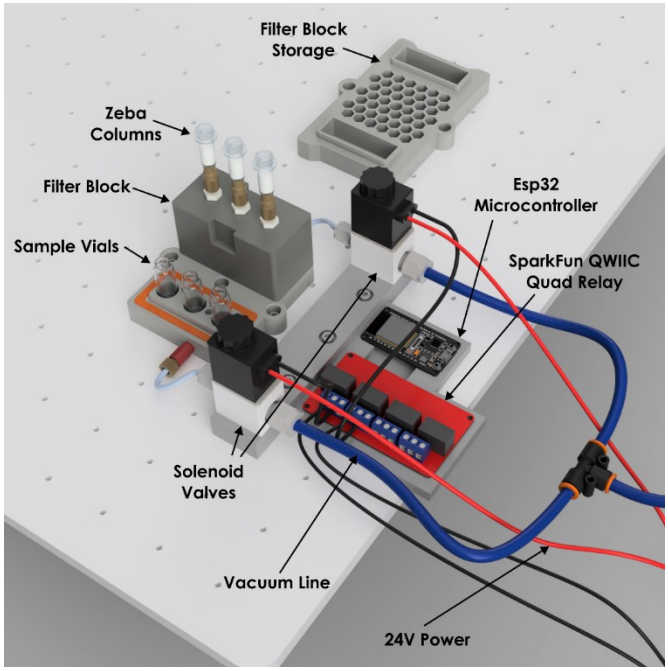

Figure S7. Top: Photo of the vacuum filtration apparatus. The solenoid (green) switches the vacuum flow between the left and right filter bases. The hollow filter block (magenta) connects the gel filtration column with the waste and HPLC vials. The base (blue) held the waste and HPLC vials. Bottom: Render of the vacuum filtration apparatus showing the full layout of the component.

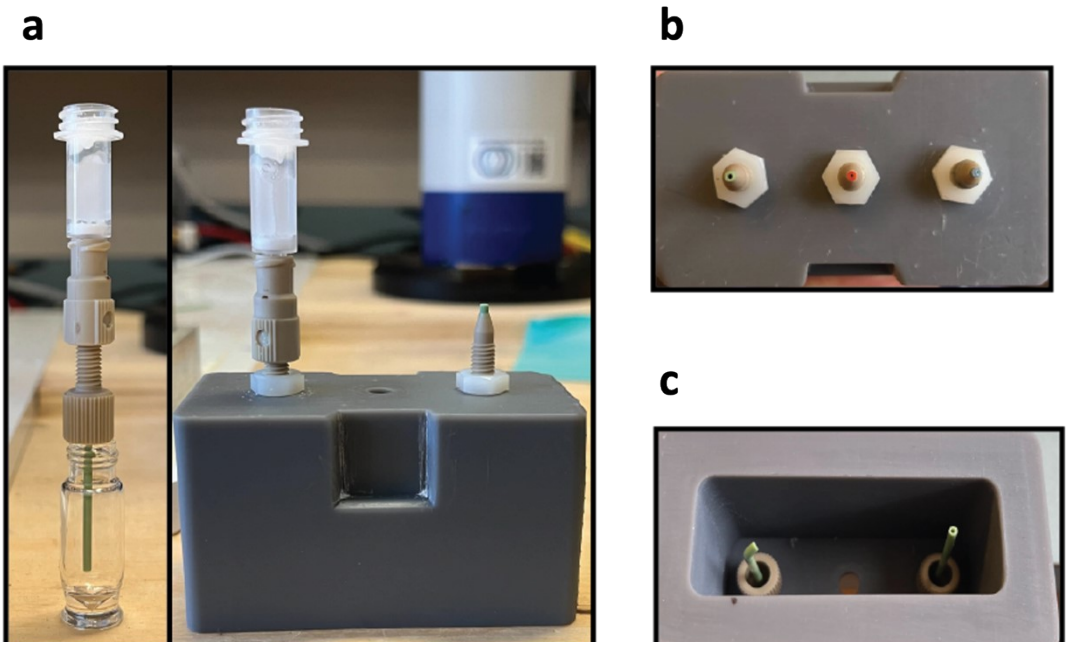

Figure S8. Filtration block components. (a) The components in the filtration block that connected the filtration column to the HPLC vial, (b) the tube inner diameters that were tested during the development of the vacuum filtration apparatus (from left to right: 0.03-, 0.02-, and 0.01-inch ID), and (c) the curved and straight tubes that were tested. The optimal setup was found to be the 0.03-inch ID tubing with a curve at the base.

A bend in the connecting tube was mechanically introduced to prevent liquid splatter and sample contamination during vacuum filtration. By pointing the tube to the side, air no longer disturbed the liquid at the bottom of the vial, decreasing splatter (Table S2). Instead, liquid was expelled towards the side, trickling undisturbed to the bottom. The bend in the tube also prevented storage solution and PBS waste from adhering to the tube during the rounds of column equilibration, eliminating contamination of the purified solution.

Test Number	1	2	3	4	5	6
Tube Inner Diameter (inches)[a]	0.03	0.03	0.01	0.02	0.02	0.03
Vacuum Strength (mbar)	400	600	600	400	200	600
Vacuum Time (s)	30	60	60	60	30	60
Curved Tube[b]	No	No	No	No	No	Yes
Waste Splatter	Yes	Yes	No	No	No	No
Antibody Yield (%)[c]	76	81	0	48	30	58

Table S2. Automatic vacuum filtration method development.

All tests were run without replicates. [a, b]See ESI Fig. 6 for details of the different tube shapes. [c]Drug-linker yield was less than 1% for all tests.

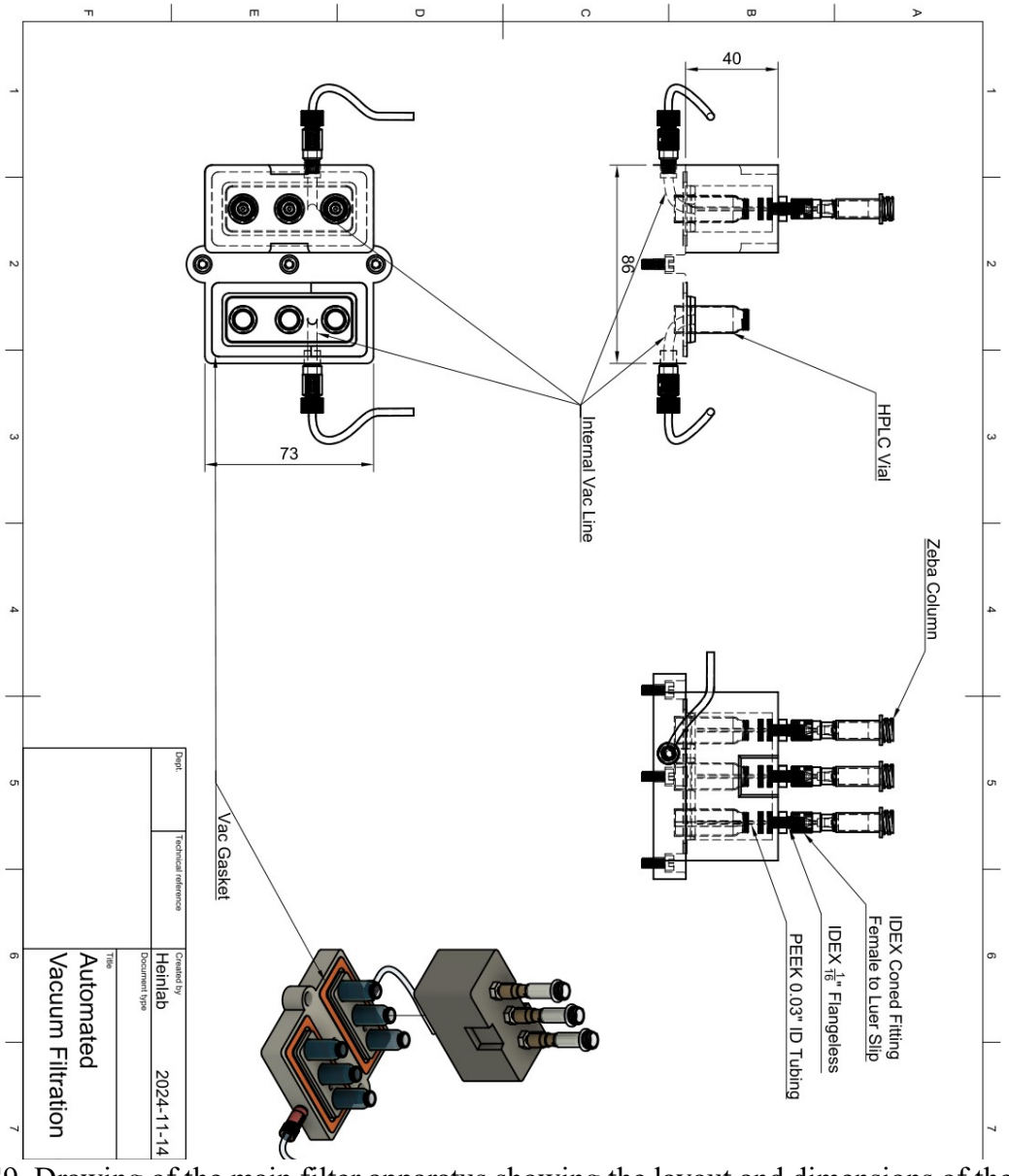

Figure S9. Drawing of the main filter apparatus showing the layout and dimensions of the device.

Capper / Decapper

HPLC

Figure
compre

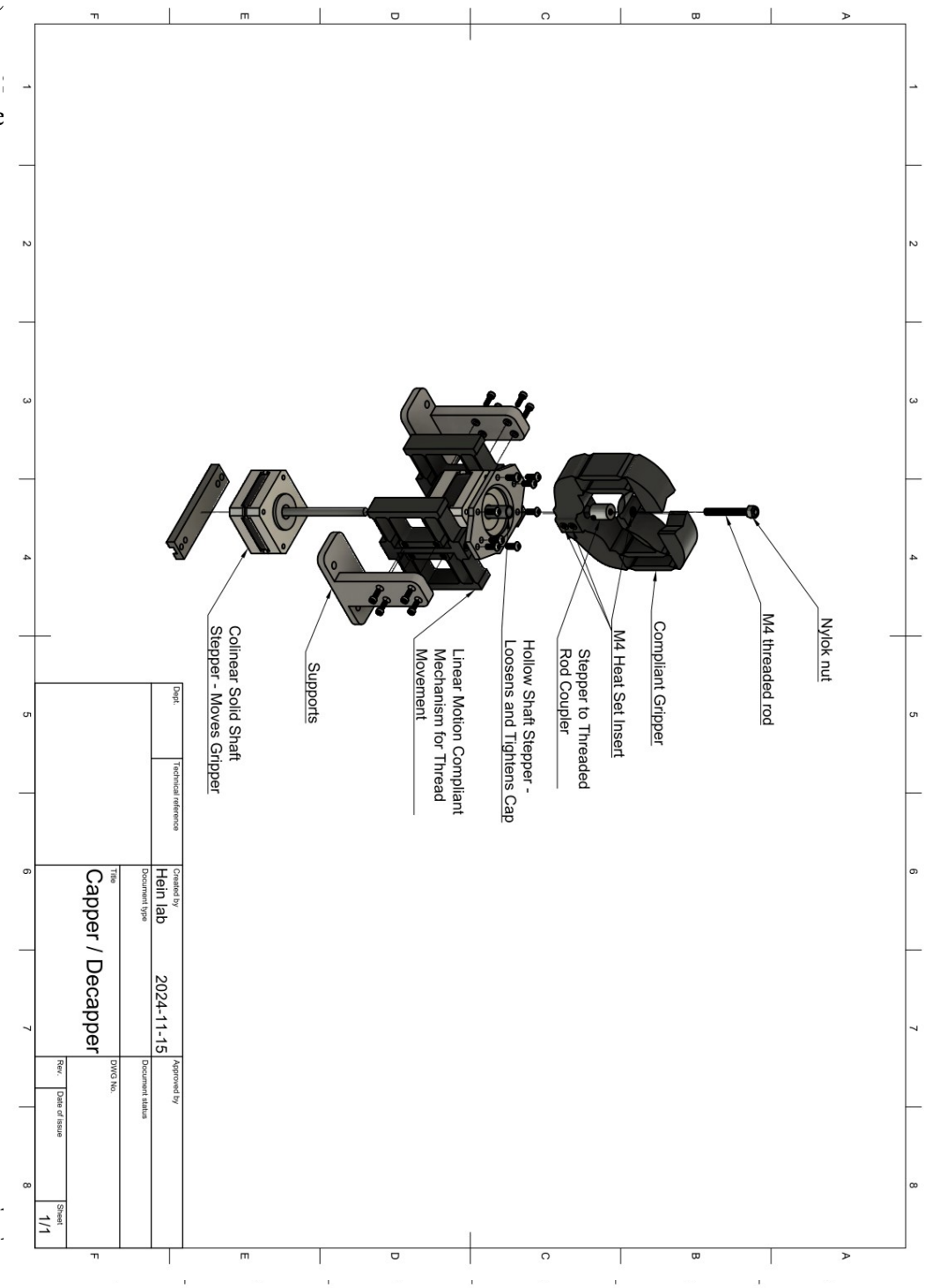

Ana

Figure S10. Exploded view of the components of the capper / decapper showing the colinear stepper design. The upper stepper motor has a hollow shaft to turn the gripper. The lower stepper has a shaft that goes through the hollow shaft to open and close the gripper.

HIC-HPLC

We analyzed the antibody-drug conjugates (ADCs) using this HIC-HPLC method, which effectively separates the different drug-to-antibody ratio (DAR) species and allows for the calculation of the average DAR.

Column	TSKgel Butyl-NPR 2.5 µm PS C4, 35 x 4.6 mm	
Column Temperature	25 °C	
Flow Rate	0.500 mL/min	
Injection Volume	20 µL	
Detection	190 - 400 nm	
Acquisition Time	Run time: 12.00 min Post run time: 5.50 min	
Mobile Phases	Solvent A: 1.5 M ammonium sulfate, 25 mM sodium phosphate monobasic, pH 6.5 Solvent B: 75% 25 mM sodium phosphate monobasic, 25% 2-propanol, pH 6.5	
Mobile Phase Program	Time (min): 0.00 12.00	%B: 5 95

The DAR was determined by multiplying the area of each DAR species peak by the number of conjugated drugs, summing these products, and then dividing by the total area of the DAR species peaks. These calculations are summarized in the formula below.

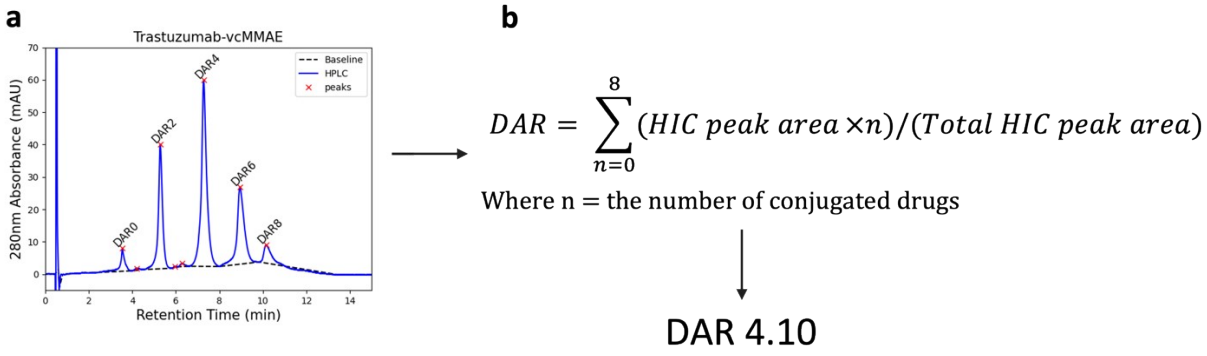

Figure S12. DAR calculation. (a) An example of an ADC HIC-HPLC absorbance plot at 280 nm and (b) the formula used to calculate the average DAR of an ADC.

UV-Vis spectrophotometry

UV-Vis spectrophotometry was used to determine the yields of the antibody and drug-linker during the development of the automated vacuum filtration module. A solution containing either Trastuzumab or vcMMAE was analyzed using a droplet UV-Vis spectrophotometer both before and after purification. The yield was calculated by comparing the absorbance before and after purification at their respective maximum absorbance wavelengths (Trastuzumab: 280 nm, vcMMAE: 248 nm).

$$\%\ Purification\ yield = 100\% \times \left(\frac{Absorbance\ after\ purification}{Absorbance\ before\ purification}\right)$$

Experimental procedures

Automated antibody-drug conjugation

The following procedure was used for the automated conjugations that yielded the results presented in this paper. It was developed based on both manual conjugation and the initial automated conjugation protocols.

1. Manually placed reduction reagents (TCEP, Trastuzumab, DTPA, and PBS) and filter blocks with gel filtration columns on the automation deck.

2. The robotic arm transferred an uncapped HPLC vial from a tray to the gravimetric balance.

3. The robotic arm picked up the liquid handler.

4. The liquid handler sequentially added the following reagents to the HPLC vial, with reagent weights verified by the gravimetric balance to determine actual quantities:

   i) 4.2 mg/mL Trastuzumab

   ii) 0.2 mM TCEP

   iii) 5 mM DTPA (to achieve a final concentration of 1 mM DTPA)

   iv) PBS pH 7.4 (to dilute the antibody to 1.13 mg/mL)

5. The robotic arm moved the HPLC vial to the custom-built HPLC vial Capper, where it was capped.

6. The robotic arm transferred the capped vial to the thermo-shaker.

7. The reduction reaction proceeded for 3 hours at 37°C.

8. Excess TCEP was removed using the automated vacuum filtration method.

9. The robotic arm transferred the new HPLC vial containing reduced and purified Trastuzumab to the gravimetric balance.

10. Prior to the conjugation step, 1 mM vcMMAE was manually mixed in a 1:3 ratio with PBS pH 7.4 to produce a 0.25 mM vcMMAE solution

11. The robotic arm picked up the liquid handler and it added excess equivalents of 0.25 mM vcMMAE.

12. The vial was capped like before and brought to the thermo-shaker for a 2-hour reaction at 25°C.

13. Excess vcMMAE was removed using the automated vacuum filtration method.

14. Manually transferred the new HPLC vial containing the purified Trastuzumab-vcMMAE ADC to the HIC-HPLC for DAR analysis.

Automated vacuum filtration

The following procedure was used for the automated conjugations that yielded the results presented in this paper. It was developed based on the multiple rounds of method development described in this paper.

1. The robotic arm securely held the filtration block on the left filtration base while the pump applied 600 mbar of vacuum for 60 seconds to expel the storage solution of the 0.5 mL 40K Zeba gel filtration column into a waste vial.

2. The robotic arm brought the liquid handler to the filtration block, and 300 µL of PBS pH 7.4 was dispensed into the filter column to equilibrate it.

3. The robotic arm secured the filtration block while the pump applied 600 mbar of vacuum for 60 seconds.

4. The filter column equilibration and vacuum application were repeated two more times.

5. The robotic arm transferred the liquid handler to the unfiltered reduced antibody or ADC (depending on the conjugation step) within the HPLC vial placed in the thermo-shaker.

6. The liquid handler aspirated the unfiltered solution, and the robotic arm returned the liquid handler to the filter block, where it dispensed the solution into the equilibrated column.

7. The robotic arm transferred the filtration block to the right filtration base, which held a clean HPLC vial.

8. The pump applied 600 mbar of vacuum for 60 seconds to the right filtration base (the application of vacuum to the left or right filtration base was controlled by a custom-built solenoid valve).

9. Upon completion of filtration, the robotic arm relocated the filtration block to an open tray.

SDL method development

Manual antibody-drug conjugation

To minimize antibody usage during the development of the automated conjugation platform, we used a low antibody concentration of 1.13 mg/mL. Following the conjugation method outlined below, three ADCs were produced with good reproducibility (standard deviation = 0.08) (Table S3).

1. To Trastuzumab, we added 4.5 equivalents of 0.2 mM TCEP and 5 mM DTPA (to achieve a final concentration of 1 mM DTPA).

2. PBS pH 7.4 was added to reach an antibody concentration of 1.13 mg/mL.

3. The reduction reaction was carried out for 3 hours at 37°C.

4. Excess TCEP was removed with 0.5 mL 40K Zeba columns following the standard procedure.[1]

5. A 1 mM vcMMAE solution was mixed in a 1:1 ratio with PBS pH 7.4 to achieve a concentration of 0.5 mM vcMMAE.

6. To the reduced Trastuzumab, we added 12 equivalents of 0.5 mM vcMMAE, and the conjugation reaction was allowed to proceed for 2 hours at room temperature.

7. Excess vcMMAE was removed with 0.5 mL 40K Zeba columns following the standard procedure.

8. Finally, the purified Trastuzumab-vcMMAE ADCs were analyzed using HIC-HPLC.

The strong reproducibility of DAR between replicates, as shown in Table S3, suggested that the low antibody concentration used in this procedure was unlikely to cause reproducibility issues when adapted for automated conjugations.

Table S3**.** DAR reproducibility between manually conjugated ADCs.

Conjugation	1	2	3
Reduction Time (hr)	3	3	3
TCEP Equiv	4.5	4.5	4.5
DAR	3.96	4.10	4.14
Standard Deviation	0.08		

Initial automated antibody-drug conjugation

The initial automated conjugation was adapted from the manual procedure and followed the protocol outlined below.

1. Manually placed reduction reagents (TCEP, Trastuzumab, DTPA, and PBS) and filter blocks with gel filtration columns on the automation deck.

2. The robotic arm transferred an HPLC vial from a tray to the gravimetric balance.

3. The robotic arm picked up the liquid handler.

4. The liquid handler sequentially added the following reagents to the HPLC vial, with reagent weights verified by the gravimetric balance to determine actual quantities:

   i) 4.2 mg/mL Trastuzumab

   ii) 4.3 equivalents of 0.2 mM TCEP

   iii) 5 mM DTPA (to achieve a final concentration of 1 mM DTPA)

   iv) PBS pH 7.4 (to dilute the antibody to 1.13 mg/mL)

5. The robotic arm moved the HPLC vial to the custom-built HPLC vial Capper, where it was capped.

6. The robotic arm transferred the capped vial to the thermo-shaker.

7. The reduction reaction proceeded for 3 hours at 37°C.

8. Excess TCEP was removed using the automated vacuum filtration method.

9. The robotic arm transferred the new HPLC vial containing reduced and purified Trastuzumab to the gravimetric balance.

10. Prior to the conjugation step, 1 mM vcMMAE was manually mixed in a 1:1 ratio with PBS pH 7.4 to produce a 0.5 mM vcMMAE solution.

11. The robotic arm picked up the liquid handler and it added 14.2 equivalents of 0.5 mM vcMMAE.

12. The vial was capped like before and brought to the thermo-shaker for a 2-hour reaction at 25°C.

13. Excess vcMMAE was removed using the automated vacuum filtration method.

14. Manually transferred the new HPLC vial containing the purified Trastuzumab-vcMMAE ADC to the HIC-HPLC for DAR analysis.

The initial attempt at automated conjugation closely followed the manual conjugation method; however, no conjugation occurred (Figure S13). This was likely caused by insufficient phase mixing between the 0.5 mM vcMMAE solution (50% DMSO) and the aqueous Trastuzumab solution, as the automated liquid handler lacked the ability to mix the solutions through continuous pipetting, as was done manually. To improve phase mixing in future automated conjugations, we diluted vcMMAE in PBS pH 7.4 to 0.25 mM (25% DMSO).

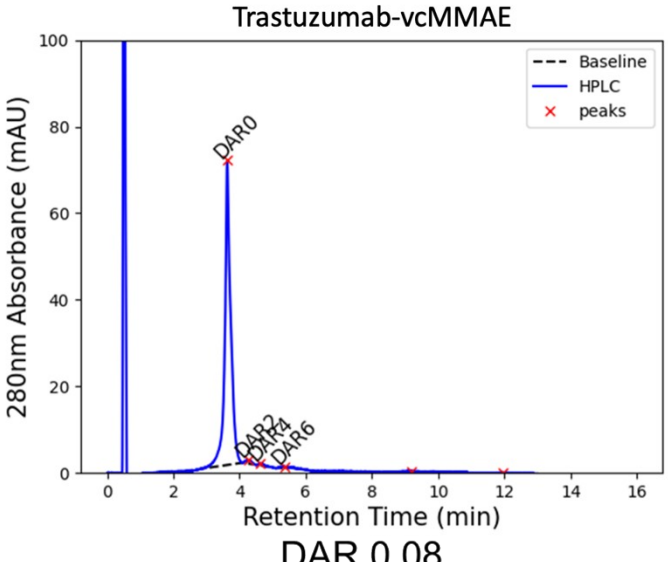

Figure S13. Initial automated conjugation. HIC-HPLC plot of the first round of automated conjugation showed negligible conjugation occurred.

SDL architecture

Python script organization

To regulate each component on the automation deck, we developed Python functions that communicated with the individual components via serial ports. To ensure a structured and coherent Python script, we started by creating low-level functions that performed simple commands like ‘close gripper’ and 'move needle’ (Figure S14). Next, we compiled mid-level functions, which combined a series of low-level functions to execute tasks such as ‘reagent addition’ and 'cap vial’. After establishing the mid-level functions, we developed high-level functions. An example of a high-level function for the system was ‘antibody reduction’, which incorporated a sequence of mid-level functions to complete the entire antibody reduction reaction. With the high-level functions in place, a conjugation reaction could be autonomously executed by invoking four functions.

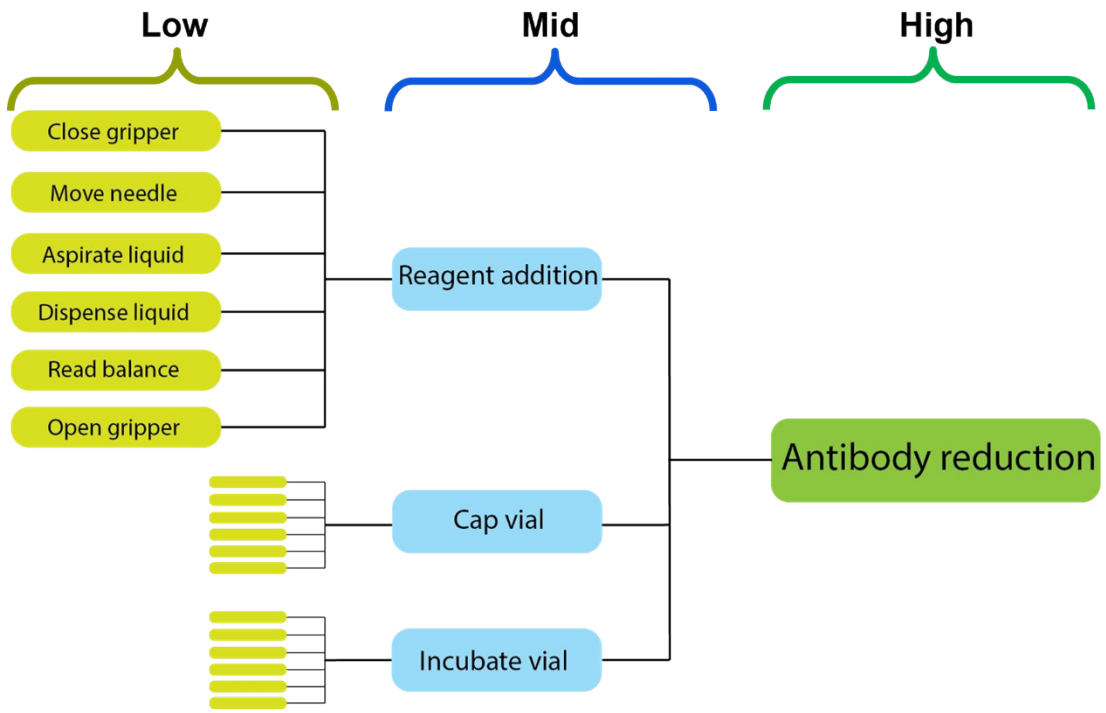

Figure S14. Hierarchical organization of functions in the automation platform’s Python script.

Gravimetric correction

To improve the liquid handler’s accuracy, we integrated a gravimetric balance into the deck and added a decision point for the automation system to correct reagent additions based on the

measured reagent weight (Figure S15). If the initial volume determined by the balance was below the intended volume, depending on the required accuracy, the system performed a second reagent addition. Also, knowing the real antibody and TCEP volumes allowed the automation system to calculate the actual TCEP equivalents of the reaction, which improved the accuracy of the post-conjugation DAR versus TCEP equivalents linear approximation. These gravimetric corrections helped compensate for the limited accuracy of the liquid handler.

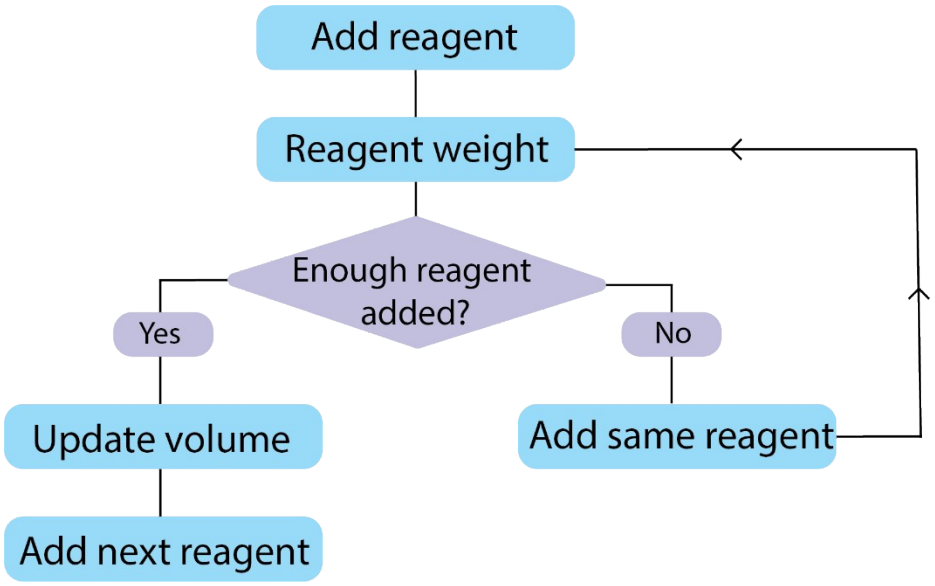

Figure S15. Gravimetric decision-tree. Outline of the automated conjugation system's liquid handling decision-making based on reagent weight.

DAR determination algorithm

DAR assignment pseudocode

Below is a simplified version of the algorithm we developed to automatically determine an ADC's drug-to-antibody ratio based on its HIC-HPLC chromatogram.

Algorithm 1 DAR assignment

INPUT: peaks, dl_ab_ratio, peak_height, retention_time

SELECT peaks, retention_time, peak_height **WHERE** dl_ab_ratio< 1.2
SELECT top 5 peaks, retention_time **BY** peak_height
IF retention_time[0] < 4 minutes **THEN**
  SET initial DAR_values to [0, 2, 4, 6, 8]
ELSE
  SET initial DAR_values to [2, 4, 6, 8]
WHILE LEN(peaks) > 2
  Perform linear regression on DAR_values vs. dl_ab_ratio
  IF R^2 < 0.99 **THEN**
    Remove the peak with the smallest peak_height
  ELSE
    Calculate DAR for all peaks using linear fit equation
    Round predicted DAR to the nearest valid even integer (0, 2, 4, 6, 8) or -1
    IF exist(duplicate DAR assignment) **THEN**
      SET DAR of smaller peak height to -1
    OUTPUT final DAR assignment
ELSE
  OUTPUT no DAR assignment

Figure S16. Pseudocode of DAR assignment from HIC-HPLC data.

Custom peak integration

To facilitate the integration of 280 nm absorbance peaks, the DAR determination algorithm utilized a series of four complementary functions, three of which came from the Python libraries SciPy and NumPy. These functions manipulated the HIC-HPLC data through various mathematical operations.

1. The SciPy savgol filter function smoothed the HIC-HPLC 280 nm absorbance plot to prepare it for derivation.[2]

2. The NumPy gradient function approximated the first derivative of the HIC-HPLC 280 nm absorbance plot to identify peak endpoints.[3]

3. A custom function identified peak boundaries by detecting local minima, specifically points where the first derivative transitioned from negative to positive (Figure S17b). This approach was chosen over selecting peak boundaries based on where the absorbance reaches zero due to the lack of a definitive baseline in the HIC-HPLC plots (Figure S18 and S19).

4. Once the peak start and endpoints were identified, the SciPy simps function integrated the area between these boundaries, which facilitated the calculation of the ADC's average DAR (Figure S12).[4]

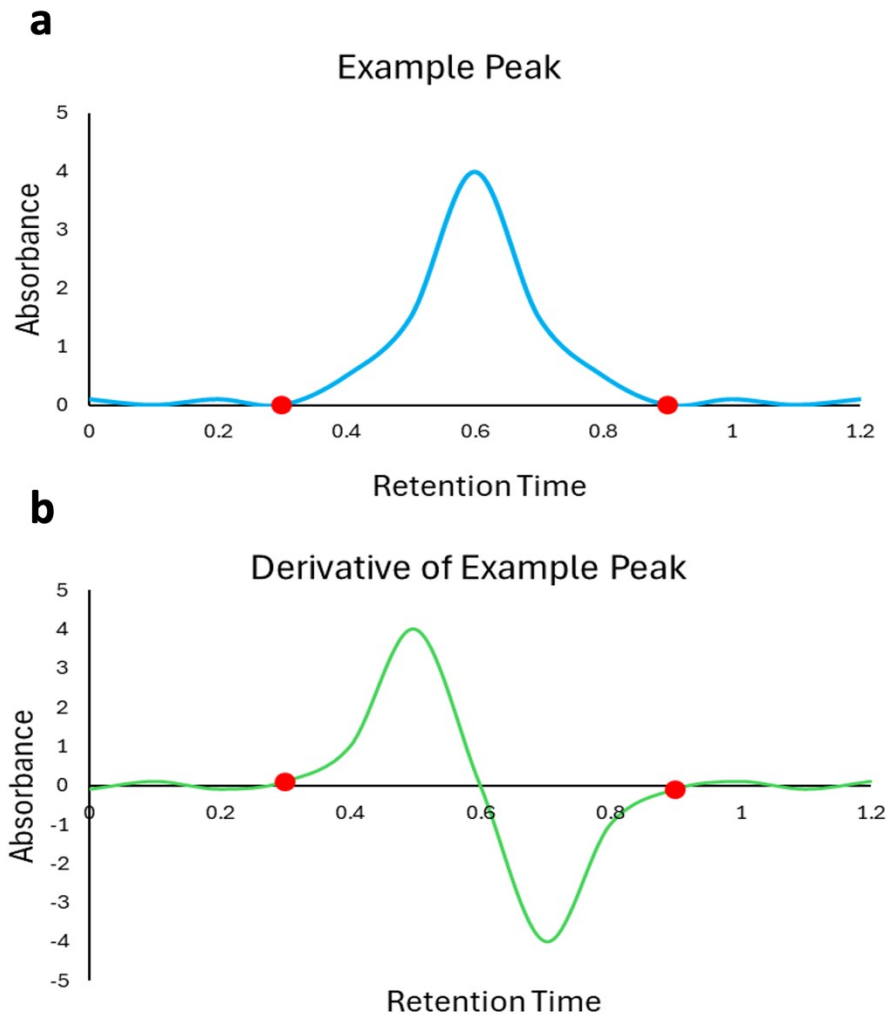

Figure S17. Tangential skimming with first derivative. (a) The start and endpoints of a peak were determined by (b) the location of a transition from a negative to a positive first derivative value.

Expanded data

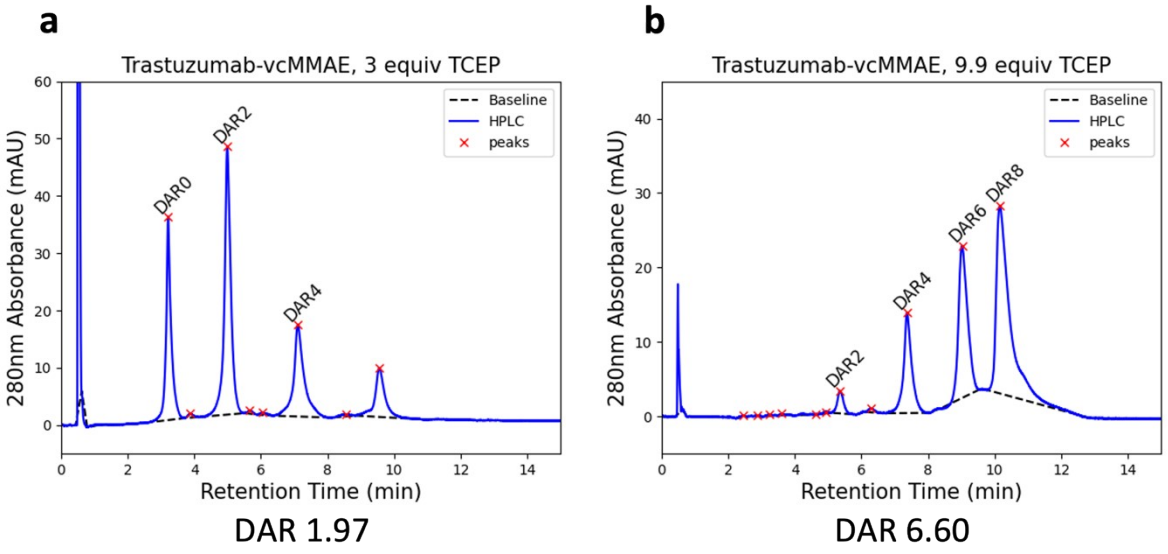

Figure S18. The DAR range of the algorithm. (a-b) The HIC-HPLC plots show the algorithm's ability to analyze ADCs across a wide spectrum of average DAR values. (a) The significant peak at 9.6 min corresponds to unpurified vcMMAE.

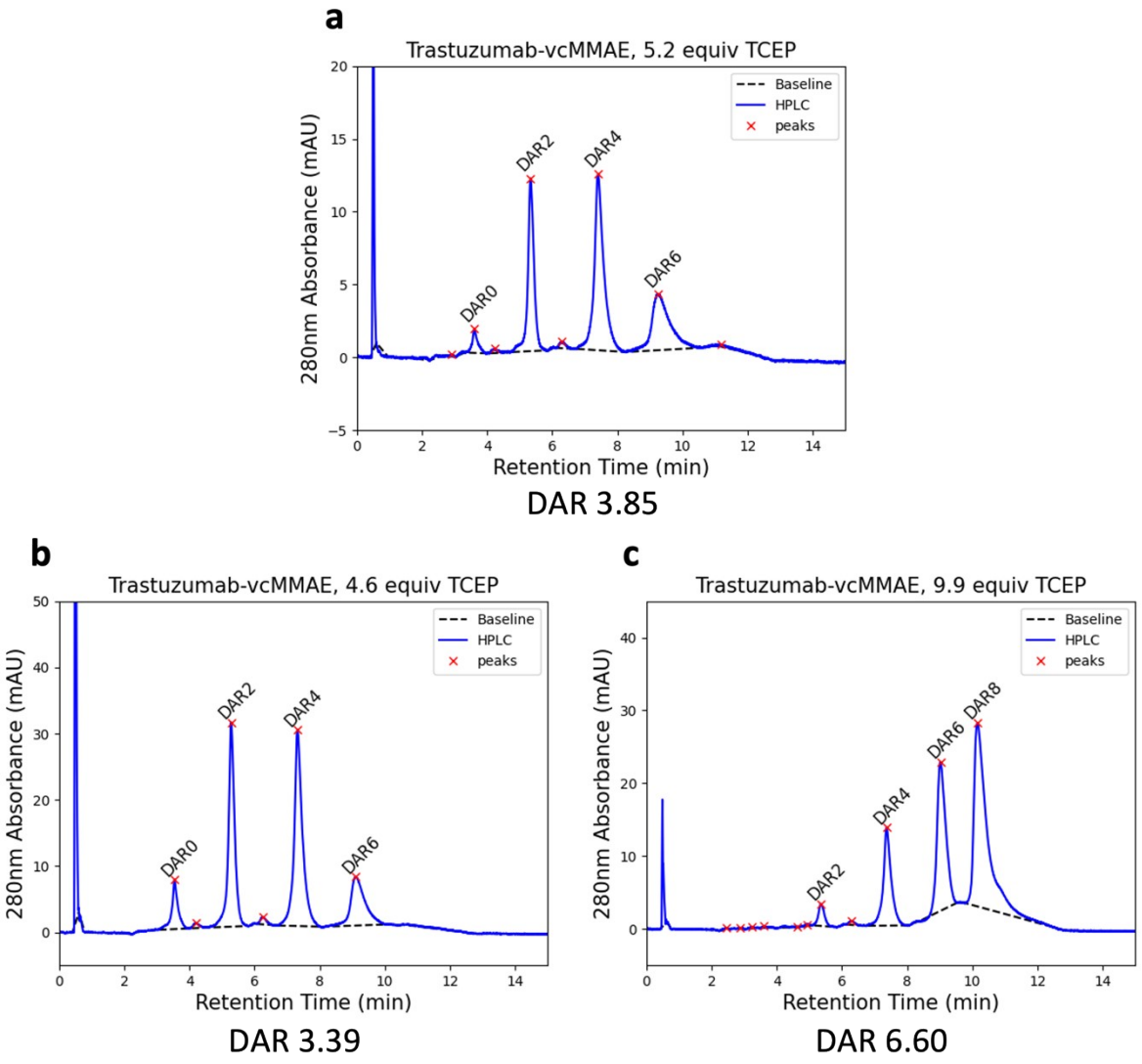

Figure S19. Automated stochastic conjugations. (a-c) These HIC-HPLC plots demonstrate the platform can automatically conjugate and characterize ADCs.

References

1 Zeba™ Spin Desalting Columns and Plates, 40K MWCO, 75 µL–10 mL, https://www.thermofisher.com/order/catalog/product/es/en/A57756, (accessed 14 June 2024).

2 scipy.signal.savgol_filter — SciPy v1.13.1 Manual, https://docs.scipy.org/doc/scipy/reference/generated/scipy.signal.savgol_filter.html, (accessed 14 June 2024).

3 numpy.gradient — NumPy v1.26 Manual, https://numpy.org/doc/stable/reference/generated/numpy.gradient.html, (accessed 14 June 2024).

4 scipy.integrate.simps — SciPy v0.14.0 Reference Guide, https://docs.scipy.org/doc/scipy-0.14.0/reference/generated/scipy.integrate.simps.html, (accessed 14 June 2024).